Theory of the lattice thermal conductivity in bulk and films of GaN

A. AlShaikhi,[1] Saswati Barman,[2] and G. P. Srivastava[3]
[1]*Physics Department, Faculty of Science, King Abdulaziz University, P.O. Box 80203, Jeddah 21589, Saudi Arabia*
[2]*Department of Material Sciences, S. N. Bose National Centre for Basic Sciences, Block JD, Sector III, Saltlake, Kolkata 700098, India*
[3]*School of Physics, University of Exeter, Stocker Road, Exeter EX4 4QL, United Kingdom*
(Received 13 March 2010; revised manuscript received 2 May 2010; published 27 May 2010)

We report on a systematic theoretical investigation of the lattice thermal conductivity of several GaN samples (bulk and films) over a wide range of temperature, by applying Callaway's relaxation-time theory in its full form and Srivastava's scheme for anharmonic three-phonon scattering processes. The role of the usually neglected three-phonon normal-drift term has been quantified. We have attempted to quantify the role of phonon scattering by various defects and imperfections, present in the film samples, in controlling the temperature dependence of thermal conductivity. We find that except for the purest sample, the phonon-impurity scattering plays a significant role in controlling the thermal conductivity of GaN not only around the thermal-conductivity peak region but also over a very large range of temperature. It can also be predicted from our numerical study, and with available experimental results, that the highest possible thermal conductivity of bulk GaN can only be realized when point impurities such as oxygen and silicon are in small concentration ($\simeq 10^{16}$ cm^{-3} or less) and other defects are either absent (from experimental study) or present in very small concentration (our numerical study). The highest value of the room-temperature thermal conductivity is achieved for samples grown by the high-temperature and high-pressure growth technique.

DOI: 10.1103/PhysRevB.81.195320 PACS number(s): 65.40.−b, 63.20.kp

I. INTRODUCTION

Due to the wide range of potential applications, gallium nitride (GaN) has been receiving an extensive and growing research attention. GaN-based proposed technologies include applications in high-power electronic devices, light-emitting diodes, laser diodes, ultrapower switches, and microwave-power sources. Reliable performance of such devices depend on the heat dissipation in the active regions. Therefore, the thermal conductivity of GaN plays a key role in controlling the performance of GaN-based devices. GaN is one of the 12 "high thermal conductivity" nonmetallic materials.[1] This advantage allows GaN to be an excellent candidate for device applications. Since heat conduction in semiconductors is primarily due to phonons, understanding various phonon-scattering processes in limiting the thermal conductivity of GaN is extremely important for device design and improvement of device performance. The lattice thermal conductivity of most of the semiconducting materials such as diamond, Si, and Ge is controlled by the point-impurity defect scattering around the thermal-conductivity peak region and by the anharmonic three-phonon scattering at room temperature and beyond that. In contrast, it has been found that the temperature dependence of the thermal conductivity of bulk GaN and GaN films deviates from that in most of the semiconducting materials. Due to different growth techniques used, H, Si, and Ga vacancies, unintentionally doped impurities such as oxygen, oxygen-related defects, and various other defects form sources of phonon scattering, severely limiting the thermal conductivity of GaN over a wide range of temperature. GaN films grown on foreign substrates contain structural imperfections such as dislocations due to the presence of the strain field arising from the lattice mismatch between the substrate and the film. Such imperfections also scatter the heat-carrying phonons and thereby limit the phonon thermal conduction. These extra scattering processes may become one of the main causes of different temperature dependence of the thermal conductivity of GaN as compared to other materials.

Sichel and Pankove[2] made the first measurements of the thermal conductivity of 400-μm-thick GaN film grown by hydride vapor-phase epitaxy (HVPE) in the temperature range 25–360 K and obtained the room-temperature thermal-conductivity value $\sim$130 W m^{-1} K^{-1} along the c axis. Asnin *et al.*[3] measured the room-temperature thermal-conductivity value of a lateral epitaxial overgrown (LEO) GaN film using the scanning thermal microscopy technique and reported the thermal-conductivity values to be in the range 170–180 W m^{-1} K^{-1}. Using the third harmonic electrical (3ω) technique, Luo *et al.*[4] found the room-temperature thermal conductivity of $\sim$155 W m^{-1} K^{-1} for LEO GaN of 5 μm thickness, a value significantly higher than previously reported for bulk GaN. This is believed to be due to substantially lower amount of dislocation density in the LEO film (less than 5×10^{6} cm^{-2}).[4] In comparison, the HVPE-grown GaN films usually have higher dislocation density on the order of 10^{10} cm^{-2}. In a following work, Luo *et al.*[5] presented results for the thermal conductivity of LEO GaN over the temperature range 60–300 K. Kamano *et al.*[6] measured the thermal conductivity of bulk GaN in the temperature range 110–370 K by photothermal divergence method and predicted that the phonon-defect scattering may play a crucial role near the room temperature. In 2002, Slack *et al.*[7] employed the steady-state heat-flow technique to measure the thermal conductivity of a 200-μm-thick and 3000-μm-wide GaN sample prepared by the HVPE technique and reported the room-temperature value as 227 W m^{-1} K^{-1}. Jeżowski *et al.*[8–10] have measured the

thermal conductivity of highly conducting *n*-type samples and highly resistive Mg-doped bulk GaN in the temperature range 4.2–300K. For the best sample of Jeżowski *et al.*, the reported highest thermal conductivity is 1600 $W\ m^{-1}\ K^{-1}$ at 45 K. The thermal conductivity of this sample is much superior compared to the other samples studied by Jeżowski *et al.* throughout the whole temperature range. Optical pump-probe measurements were performed by Daly *et al.*[11] to extract the thermal conductivity of polycrystalline GaN films and single-crystal alloy thin films in the temperature range 150–400 K. The thermal-conductivity values for polycrystalline GaN films are much reduced compared to single-crystal GaN. Similarly, the thermal conductivity of alloy thin films are also substantially reduced compared to bulk GaN. Liu and Balandin[12] carried out measurements of the thermal conductivity of a 18.5-μm-thick GaN film and a 0.7 μm AlGaN alloy film using the differential 3ω technique. Their measurement shows an unusual temperature dependence for the conductivity of the alloy films.

Theoretically, the room-temperature thermal-conductivity value of 170 $W\ m^{-1}\ K^{-1}$ for a perfect GaN crystal was predicted by Slack.[1] Later in 2002, Slack *et al.* in 1973 (Ref. 7) predicted a pure GaN single crystal to have a room-temperature thermal-conductivity value of 250 $W\ m^{-1}\ K^{-1}$. Witek[13] calculated the room-temperature thermal conductivity of GaN to be 410 $W\ m^{-1}\ K^{-1}$. According to Witek,[13] the discrepancy between his result and previously reported values is attributed to impurities and defects. In his opinion, the most effective phonon scatterings at the room temperature in GaN and AlN are the lattice defect scattering and in BN are the isotope scattering. Theoretical calculation of the thermal resistivity by Berman[14] supports the view expressed by Witek. Kotchetkov *et al.*[15] and Zou *et al.*[16] have extensively calculated the effect of dislocation and isotope scattering in GaN. Kamatagi *et al.*,[17] using a slightly different form[18] of the Callaway model,[19] have presented a systematic theoretical study of the thermal conductivity of GaN. However, their study is based on an *ad hoc* form of three-phonon relaxation time, containing empirically adjustable parameters.

Despite the considerable amount of work on both experimental and theoretical studies of the thermal conductivity of bulk and films of GaN, accurate estimates of the contributions of various phonon-scattering events in different ranges of temperatures in controlling the thermal conductivity is nearly absent in the literature. The main reasons for this are the poor understanding of three-phonon umklapp processes and normal (N) processes, and a complete negligence of the N-drift term in the evaluation of Callaway's conductivity expression. In all previous works on thermal conduction in GaN, including the work by Kamatagi *et al.*,[17] the phonon relaxation rate for umklapp and normal processes have been treated in an *ad hoc* manner and several adjustable parameters are present in the expression for three-phonon anharmonic relaxation rate. In some cases, the contribution of normal processes are completely neglected. In earlier work on thermal conductivity of Ge,[20] Srivastava used the full form of Callaway's expression with an expression for the three-phonon anharmonic interaction derived systematically from the anharmonic continuum theory[21] and showed that the N-drift term provides a significant contribution. In recent studies on thermal conductivity of diamond,[22] GaAs nanobeam,[23] and AlN,[24] the authors have shown that the contribution of the N-drift term can be as high as 50% of the total conductivity result.

In this paper, we have employed Srivastava's expression for the three-phonon scattering rate containing Grüneisen's constant as the single adjustable parameter for all allowed three-phonon processes.[21] With these expressions, we systematically include the contribution from the N-drift term in Callaway's expression for thermal conductivity.[19] The theory is applied to explain the experimental measurements of the thermal conductivity of bulk GaN and GaN films of different thicknesses grown under different conditions using different techniques. We have quantified the role of different phonon-scattering mechanisms including the impurity scattering in limiting the thermal conductivity over a large range of temperature.

II. THEORY

The phonon transport in thick semiconductor films, such as those studied in this work, is well described from a solution of the Boltzmann equation. The Boltzmann equation satisfied by the phonon distribution function has been solved either by applying variational methods or by assuming the concept of phonon relaxation time.[21]

A. Callaway's expression for thermal conductivity

The most famous relaxation-time expression for the lattice thermal conductivity is due to Callaway.[19] A generalized version of Callaway's expression can be written, within the isotropic continuum model, as[21]

$$K_C = \frac{\hbar^2 q_D^5}{6\pi^2 k_B T^2}\left[\sum_s c_s^4 \int_0^1 dx x^4 \tau \bar{n}(\bar{n}+1) + \frac{\left\{\sum_s c_s^2 \int_0^1 dx x^4 \tau \tau_N^{-1} \bar{n}(\bar{n}+1)\right\}^2}{\sum_s \int_0^1 dx x^4 \tau_N^{-1}(1-\tau\tau_N^{-1})\bar{n}(\bar{n}+1)}\right], \quad (1)$$

$$= K_D + K_{\text{N-drift}}, \quad (2)$$

where c_s is the phonon speed for polarization branch s, $\bar{n}$ is the Bose-Einstein distribution function, q_D is the Debye radius, $x=q/q_D$ is the reduced wave vector, τ is the phonon relaxation time, and τ_N is the phonon relaxation time due to normal phonon-phonon scattering processes. The first and second terms in the above expression represent the Debye term K_D and the N-drift term $K_{\text{N-drift}}$, respectively. $K_{\text{N-drift}}$ represents a contribution originating from momentum-conserving nature of three-phonon N processes.

B. Expressions for relaxation time

The lifetime (τ) of a phonon is controlled by its interaction with other phonons, grain boundaries, walls of the crystal, chemical impurities, vacancies, dislocations, isotopes, and charge carriers. Assuming independence of these interaction processes, we can write within the Matthiessen's rule, $\tau^{-1}=\Sigma_i \tau_i^{-1}$, where τ_i^{-1} is the contribution from the ith process. For the GaN samples studied here, we consider the following forms.

For boundary scattering,

$$\tau_{bs}^{-1}=\frac{c}{L}, \tag{3}$$

where c is the phonon speed and L is the phonon mean-free path determined by the crystal size.

Phonon scattering by grain boundary can be expressed as[25]

$$\tau_{\text{GB}}^{-1}=B_{\text{GB}}\omega^2, \tag{4}$$

where B_{GB} is the grain-boundary coefficient if the spacing between dislocations is much smaller than the phonon wavelength, and as[25]

$$\tau_{\text{GB}}^{-1}=B_{\text{GB}}\omega^n, \tag{5}$$

where $0\leq n\leq 1$, if the spacing between dislocations is larger than the phonon wavelength. However, for the systems under study in this work, the minimum phonon wavelength is larger than grain sizes so phonon relaxation rate due to grain-boundary scattering has been calculated using Eq. (4).

For isotopic mass-defect scattering,

$$\tau_{\text{md}}^{-1}=\frac{\Omega\Gamma}{4\pi\bar{c}^3}\omega^4 = A\omega^4, \tag{6}$$

where Ω is the volume of a unit cell, $\bar{c}$ is the average phonon speed, and $\Gamma=\Sigma_i f_i\frac{\delta M_i}{\bar{M}}$ is the mass-defect scattering parameter. f_i is the percentage of ith isotope present in the crystal, $\bar{M}$ is the average atomic mass of all the isotopes present in the crystal, $\delta M_i=|M_i-\bar{M}|$, where M_i is the mass of ith isotope. Phonon scattering from other kinds of point defects can be included by a suitable choice of the parameter A. In GaN film samples grown by the HVPE or high-temperature and high-pressure (HT/HP) technique, phonons can also be scattered from the agglomerates of point defects (vacancies or interstitials) such as V_{Ga}-O_N, Mg-O, or Mg-V_N complexes, and grain boundaries. Such extended-sized defects can scatter small wavelength phonons geometrically (i.e., such as boundaries) and long-wavelength phonons such as point defects (i.e., Rayleigh-type). These two possibilities can be expressed as[26,27]

$$\tau_{\text{aggregate}}^{-1}=\begin{cases} n\pi d^6\omega^4/4c^3 & \text{for } qd<1, \\ nc\pi d^2/4 & \text{for } qd\geq 1, \end{cases} \tag{7}$$

where d is the effective diameter of the defect region and n is the concentration of the aggregates.

For low donor or acceptor concentration, the phonon relaxation rate due to scattering from carriers (electrons or holes) can be expressed as[28]

$$\tau_{c\text{-ph}}^{-1}=\frac{n_c\eta^2\omega}{\rho c_s^2 k_B T}\sqrt{\frac{\pi m^* c_s^2}{2k_B T}}\exp\left(\frac{-m^*c^2}{2k_B T}\right), \tag{8}$$

where n_c is the charge-carrier density, η is the deformation potential, and m^* is the charge-carrier effective mass.

While considering phonon-phonon interaction we will restrict ourselves to only three-phonon processes. Since the scattering rate for four-phonon processes is two to three orders of magnitude smaller than that for three-phonon processes,[29] the contribution of four-phonon processes toward the conductivity is insufficient compared to three-phonon processes. We consider the three-phonon relaxation rate of a phonon in mode $(\mathbf{q},s)$ in Srivastava's scheme[21] as

$$\tau_{\mathbf{q}s}^{-1}(3\ \text{ph})=\frac{\hbar q_D^5\gamma^2}{4\pi\rho\bar{c}^2}\sum_{s's''\epsilon} c_s c_{s'}\left[\int dx' x'^2 x''_+\{1-\epsilon+\epsilon(Cx+Dx')\}\frac{\bar{n}_{\mathbf{q}'s'}(\bar{n}''_+ +1)}{(\bar{n}_{\mathbf{q}s}+1)}+\frac{1}{2}\int dx' x'^2 x''_-\{1-\epsilon+\epsilon(Cx-Dx')\}\frac{\bar{n}_{\mathbf{q}'s'}\bar{n}''_-}{\bar{n}_{\mathbf{q}s}}\right].$$

Here $x'=q'/q_D$, $x''_\pm=Cx\pm Dx'$ and $\bar{n}''_\pm=\bar{n}(x''_\pm)$, $C=c_s/c_{s''}$, $D=c_{s'}/c_{s''}$, $\epsilon=1$ for momentum-conserving (normal or N) processes, and $\epsilon=-1$ for momentum nonconserving (umklapp or U) processes. The first and second terms in the above equation are contributed by class 1 events $\mathbf{q}s+\mathbf{q}'s'\rightarrow\mathbf{q}''s''$ and class 2 events $\mathbf{q}s\rightarrow\mathbf{q}'s'+\mathbf{q}''s''$, respectively. The integration limits on the variable x' for the various combinations of the polarization branches s, s', and s'' of the three phonons involved in the interactions have been presented in Ref. 21. In the above expression, we have expressed three-phonon inter-

TABLE I. Constants used in the calculation of the thermal conductivity of GaN.

Mass density: $\rho=6.15\times10^3$ kg m^{-3}
Lattice constant: $a=4.52$ Å
Longitudinal phonon velocity: $c_L=6.9\times10^3$ m s^{-1}
Transverse phonon velocity: $c_T=5.02\times10^3$ m s^{-1}
Electron effective mass: $m_e^*=0.2m_e$
Hole effective mass: $m_h^*=0.19m_e$
Deformation potential: $\eta=9.2$ eV.
Debye radius: $q_D=1.73\times10^{10}$ m
Debye temperature: 912 K
Grüneisen constant: $\gamma=0.9$

actions in terms of the Grüneisen constant γ, and will regard this as an adjustable parameter.

We would like to mention here that there are discrepancies in the value of γ available literature. The calculated from shell-model molecular-dynamics method varies from 0.6 to 1.05 depending upon the molar volume.[30] Witek *et al.*[7] calculated $\gamma=0.74$ from thermal-expansion data and specific-heat measurement. We have used $\gamma=0.9$ which is within the range of available value of γ. The presently chosen value is slightly different from that used ($\gamma=0.8$) in our previous work on phonon lifetime in bulk GaN.[31]

III. RESULTS AND DISCUSSION

Here we analyze the experimental results obtained for GaN samples grown under different growth conditions over a wide range of temperature. The nature and amount of defects present in these samples actually depend on both the growth condition and substrate material. In our numerical calculations, we have considered extended defect scattering in addition to isolated point impurity. The presence of grown-in extended defects in GaN single crystals grown by the HP/HT method were observed and investigated by Lefeld-Sosnowska and Frymark.[32] Their study, using x-ray projection topography, revealed three types of crystal lattice imperfections: (a) large circular defects (extended defects), (b) boundaries, dividing the crystal into two disoriented parts, or shorter lines, and (c) line defects (straight dislocations). We have performed numerical calculations for samples grown by the HVPE, metal-organic chemical-vapor deposition, and LEO methods, under high temperature and high pressure. The constants used for the present calculations are taken from Ref. 33 and are listed in Table I. The scattering parameters are listed in Table II.

For convenience, the bulk GaN sample S1 studied by Slack *et al.*,[7] the sample studied by Sichel and Pankove,[2] the sample studied by Kamano *et al.*,[6] #1 from Ref. 8, #2 from Ref. 8, #3 from Ref. 8, #4 from Ref. 8, sample 2 from Ref. 9, sample 3 from Ref. 9, the 18.5 μm film from Ref. 12, and the LEO film[5] are marked in our study as samples 1, 2, 3, 4, 5, 6, 7, 8, 9, 10, and 11, respectively.

We have summarized the available experimental measurements by various groups in Table III. The last column indicates the power n in the expression $K=AT^n$ at 300 K. From this compilation, it is clear that different samples have different values of the room-temperature conductivity. The value of n at room temperature also varies between samples. Estimation of n at room temperature is important to confirm whether the thermal conductivity at this temperature is purely governed by three-phonon scattering or not. If the total phonon-scattering rate is due to pure anharmonic scattering, n at room temperature and above room temperature should be equal to -1. In other cases, n will deviate from -1, depending upon the percentage contribution of other scattering mechanism at this temperature. Table IV shows that except for the purest quality samples, point-impurity scattering plays a major role in controlling thermal conductivity over a large range of temperature. We also note that when the point-defect concentration is high, the percentage contribution of point-impurity scattering is reasonably high throughout the whole temperature range irrespective of the presence or absence of other defects. Srivastava's scheme for three-phonon processes allows us to accurately determine the three-phonon scattering processes for a large range of temperature. As a result, we are able to accurately quantify the impurity scat-

TABLE II. Parameters used in this work.

Sample no.	Sample Ref.	L (μm)	A (10^{-46} s^3)	n_{ED} (10^{18} cm^{-3})	d_{ED} (Å)	B_{GB} (10^{-17} s)	n_c (10^{17} cm^{-3})
1	S1 of 7	500	5				
2	2	50	5	600	2.1		5
3	6	0.17	11.5				1
4	#1 of 8	850	1.5	0.6	2.6	0.01	1
5	#2 of 8	100	15	12	2.15		1
6	#3 of 8	170	20	9	2.83		1
7	#4 of 8	1500	10	1.2	4	1.7	35
8	#2 of 10	100	1.5	0.9	3		5
9	#3 of 10	100	11	12	2.15		1
10	12	18.5	65				
11	UCSB LEO of 5	30	10				

TABLE III. Experimental measurements.

Sample No.	Ref.	Growth condition, substrate	Dimensions	Impurity-type, concentration (cm^{-3})	Carrier density (cm^{-3})	$K_{(300\ K)}$ ($W\ m^{-1}\ K^{-1}$)	K_{max} ($W\ m^{-1}\ K^{-1}$), T_{max}(K)	Power n at 300 K
1	7	HVPE, Sapphire	200 μm (thick), 3000 μm (wide)	$O(2.1\times10^{16})$, $Si(0.37\times10^{16})$		227	2000, 30	−1.22
2	2	$GaCl+NH_3$, 950 °C sapphire	$5\times2.65\times0.31$ mm^3	Grain boundary, $\sim10^{18}$	3×10^{17}	130	170, 200	−0.76
3	6	HVPESi doped (n type)	122 μm (thick)		1×10^{18}		170, 180	−0.6
4	8	High temp and pressure # 1 (n type)	$3\times0.05\times0.04-0.05$ mm^3	Mg, C, H, Si, O, Ga-V $\sim10^{20}$	5×10^{19}	230	1600, 45(#1)	~-1.43
5		# 2 (p type)		$\sim10^{20}$		160	~500 (#2,3)	
6		# 3 (p type)		$\lesssim10^{17}$				
7		# 4 HVPE layeron bulk GaN	100 μm (thick)	$\sim10^{20}$	$<10^{17}$			
8	9 and 10	#2(n type)				188	1050, 60	
9		#3(n type)				160	590, 60	
10	12	HVPE, sapphire	18.5 μm (thick)			125		
11	5	LEO (MOCVD)	5 μm	Dislocation (cm^{-2}) $\lesssim5\times10^6$	$3-5\times10^{18}$	>155	1000, 80	

tering throughout the temperature range, viz., not only for the temperature range for which experimental results are available but also beyond that.

A. Bulk GaN

Figure 1 presents the results for the thermal conductivity of the GaN sample (S1) studied by Slack *et al.*[7] This sample was grown on a sapphire substrate by HVPE and contained oxygen and silicon as major impurities which act as sources of point-defect scattering. Our calculated boundary scattering parameter of 500 μm matches with Slack's prediction and the original sample dimensions. Though there is a considerable amount of point impurities present, there is neither suggestion of the presence of extended defects nor did we need to consider these in our calculations. Our theoretical work reproduces the experimental results over the entire temperatures, and shows that the conductivity peak occurs at 30 K. The contribution of point-impurity scattering toward thermal resistivity is as high as 90% at 50 K, and is reasonably significant up to 500 K. Table III shows that the experimental measurement provides the highest thermal conductivity at

TABLE IV. Calculated percentage contribution of point-impurity scattering to the total thermal resistivity for different GaN samples grown under different growth technique.

T (K)	Sample no.										
	1	2	3	4	5	6	7	8	9	10	11
10	12.1	0.2	0.02	1.9	0.6	4.5	0.1	0.7	3.9	7.1	2.2
20	52.4	0.3	0.25	5.6	1.9	8.9	0.3	4.1	11.2	36.1	18.4
30	81.9	0.3	1.2	10.9	3.4	14.5	0.7	11.8	16.8	61.4	42.4
50	89.1	0.9	6.8	28.3	16.0	43.9	1.9	25.1	41.0	85.6	75.9
70	61.7	3.5	18.8	27.8	23.0	60.9	3.7	22.9	55.0	84.7	68.6
100	35.5	8.6	21.4	14.9	14.4	56.1	6.6	13.9	46.6	75.0	48.2
200	16.2	11.6	21.5	5.7	5.7	39.4	10.4	5.6	28.0	62.4	26.7
300	10.9	9.6	17.4	3.6	3.6	30.6	10.0	3.6	20.4	54.7	19.1
500	6.7	6.8	12.2	2.1	2.1	21.2	8.1	2.1	13.2	43.8	12.3
700	4.8	5.2	9.4	1.5	1.5	16.2	6.6	1.5	9.8	36.6	9.1
1000	3.4	3.9	7.0	1.1	1.1	12.1	5.2	1.1	7.1	29.4	6.5

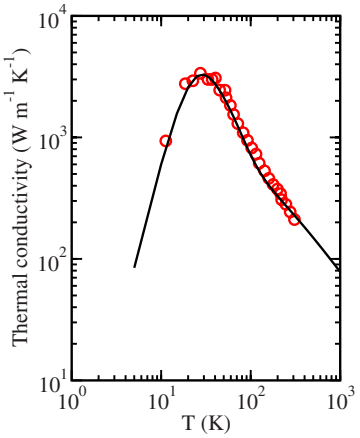

FIG. 1. (Color online) Temperature variation in the thermal conductivity of sample no. 1 [sample S1 studied by Slack *et al.* (Ref. 7)]. The solid lines represent our theoretical results and the symbols represent the experimental data for sample S1 presented in (Ref. 7).

the peak (i.e., at T_{max}) and at room temperature. Therefore, Slack *et al.*'s. sample [marked as sample 1 in the present study] can be considered to present the best value of thermal conductivity for bulk GaN.

Figure 2. shows the results for the 400-μm-thick GaN sample of Sichel and Pankove[2] [marked as sample 2 in the present study] grown by vapor-phase growth technique[34] on a 50-μm-thick sapphire substrate. Our numerical results have reasonable agreement with Sichel and Pankove's experimental results. Our fitted results of electron concentration and point-defect scattering parameter are similar to that reported in Ref. 2. However, in order to fit the experimental results at low temperatures, we had to scale the boundary scattering length to a value which is about six times smaller than the lowest dimension of the sample. This suggests that grains are present in the sample which eventually make the boundary scattering length smaller than the original dimension of the sample. We find that the effective grain size is 50 μm. Our calculations also show that the extended defect concentration is very high. This is consistent with the expected amount of defects to be present in samples grown by the vapor-phase growth technique. Table III shows that the thermal conductivity at room temperature is smaller than that of other samples studied here, and also the conductivity peak occurs at a higher temperature compared to other samples. Therefore, it is clear that the presence of large amount of defects is responsible for the attenuation of the value of thermal conductivity and the shifting of T_{max} toward higher temperature. Table IV shows that the contribution of point-impurity defect scattering toward the total thermal resistivity is ~10% and ~4% at 300 K and 1000 K, respectively.

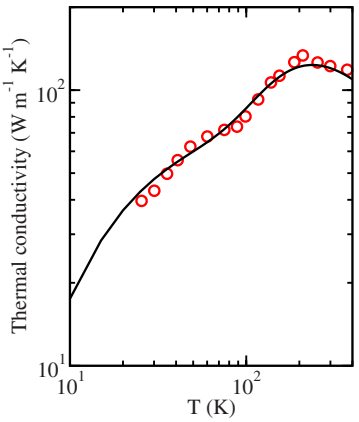

FIG. 2. (Color online) Temperature variation in the thermal conductivity of sample no. 2 (the GaN film grown by Sichel and Pankove [Ref. 2]). The solid lines represent our theoretical results and the symbols represent the experimental data presented in Ref. 2.

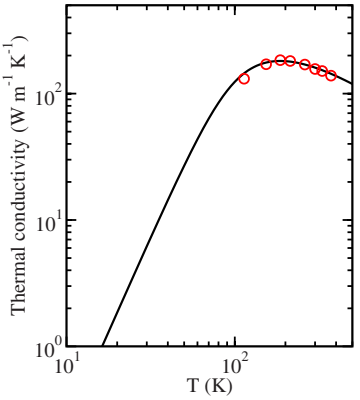

FIG. 3. (Color online) Temperature variation in the thermal conductivity of sample no. 3 (the 122-μm-thick GaN sample grown by Kamano *et al.* [Ref. 6]). The solid lines represent our theoretical results and the symbols represent the experimental data presented in Ref. 6.

Figure 3 presents the results for the 122-μm-thick GaN sample of Kamano *et al.*[6] [marked as sample 3 in the present study] along with our numerical results. In the absence of low-temperature data for this sample, it is difficult to accurately predict the boundary scattering length. However, our calculations show that the effective boundary length is very small compared to the dimension of the sample, indicating the presence of small grains inside the sample. We find that there was no extended defect in the sample. Since the sample is doped with Si, considerable amount of point defects are expected to be present in the sample. Our fitted results also indicate the same. The experimental data in Table III shows that T_{max} and K_{max} are similar for the samples studied in Refs. 2 and 6. A comparison of our calculated point-defect parameters for both the samples are similar to those expected from the experimental data.

In all the previously discussed works, GaN samples were grown on foreign substrates and the lowest temperature at which the thermal conductivity was measured was larger than 10 K. Driven by these two facts, Jeżowski *et al.*[8–10] have carried out measurements of the thermal conductivity of different GaN samples in the temperature range 4–300 K. In their work, Jeżowski *et al.*[8] have studied the thermal conductivity of four GaN samples. Sample #1, #2, #3, and #4 of Jeżowski *et al.*, are referred as sample 4, 5, 6, and 7, respectively, in the present study. The results of the thermal conductivity of these samples are presented in Fig. 4. As reported by Jeżowski *et al.*,[8–10] all the samples had the same dimensions of $3\times5\times0.04$ mm^3 (Ref. 9) [$3\times5\times0.05$ mm^3 (Ref. 10)].

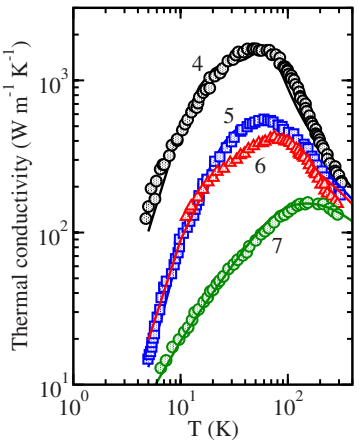

FIG. 4. (Color online) Temperature variation in the thermal conductivity of samples no. 4–7 (samples #1–#4 in the work by Jezowski *et al.* [Ref. 8]). The solid lines represent our theoretical results and the symbols represent the experimental data presented in Ref. 8.

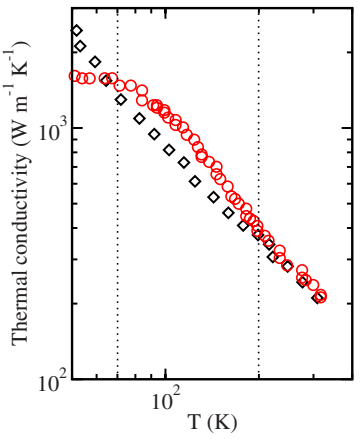

FIG. 5. (Color online) Comparison between the thermal-conductivity measurements reported in Ref. 7 for sample S1 (diamonds) with those reported in Refs. 8–10 for sample #1 (circles).

The first sample (sample #1) in Ref. 8 [sample 4 in the present study] was a highly conducting *n*-type bulk GaN crystal grown using the HP/HT method.[35] Among the four samples, this sample exhibited the best thermal conductivity. At low temperatures, the results show the T^3 behavior, indicating the dominance of boundary scattering at low temperatures. We find that the concentration of point impurities and of extended defects are small. Therefore, the impurity scattering does not significantly modify the results at room temperature and the anharmonic phonon interaction remains the dominant mechanism. In a later work,[36] the authors have extrapolated the experimental data for this sample for $T > 300$ K and compared the temperature dependence of their results at $T > T_{\max}$ with the temperature dependence of the results obtained by Mion *et al.*[37] in the temperature interval 300–450 K. They have claimed the same temperature dependence (i.e., $T^{-1.43}$) in the temperature range 200–500 K and concluded that the thermal conductivity for $T > T_{\max}$ is determined by point-defect scattering and the umklapp processes. In contrast to this conclusion, our calculations reveal that the influence of point-impurity scattering in controlling the thermal conductivity of this sample is not significant beyond 100 K.

At this point, it will be useful to draw a comparison between the results obtained from Slack and co-workers' sample [sample 1 in the present study] and Jeżowski and co-workers' best sample [sample 4 in the present study]. While these two samples provide similar values of the room-temperature conductivity, the maximum conductivity exhibited by samples 1 and 4 are, respectively, 3000 W m^{-1} K^{-1} and 1600 W m^{-1} K^{-1} at 30 and 45 K. According to our fitted results, the point-impurity content in Slack's sample is five times larger than that in Jeżowski *et al.*'s sample. This is in contrast with the reported values[8] of point-defect concentration. Jeżowski *et al.*'s samples contain very small amounts of large defect. Table IV shows that percentage contribution of point-impurity scattering toward thermal resistivity in Slack's sample is as high as 90% around the peak region. In case of Jeżowski *et al.*'s, point-impurity scattering contributes 15–28% around the peak region in. In Jeżowski *et al.*'s sample, the lower amount of point-impurity scattering is compensated by the small amount of extended defect scattering. In both samples, the N-drift contribution is saturated at around 50%. The magnitude of N-drift term is essentially controlled by the concentration of point defects.

The results for samples #2, #3, and #4 of Jeżowski and co-workers [samples 5, 6, and 7, respectively, in the present study] show a clear deviation from the T^{-1} conductivity dependence at high temperatures. Since samples #2 and #3 [samples 5 and 6] have much lower thermal conductivity compared to sample #1 [sample 4], we are interested to see the difference in defect concentration among #1 [sample 4] and (#2, #3) [samples 5 and 6]. Table II shows that both the point impurities and extended defect concentration are much higher for #2 and #3 [samples 5 and 6], compared to that for #1[sample 4]. Point impurities and extended defect concentration increase due to the Mg dopant and the formation of Mg-O complexes in #2 and #3 [samples 5 and 6].

Though our calculated results for #2 and #3 [samples 5 and 6] agree well with the experimental data at low temperatures and around the conductivity peak, the agreement is poor at higher temperatures. The experimental measurements by Jeżowski *et al.*[8] show a steeper slope compared to other experimental results[7] and our numerical calculations. The concentration of point impurities and boundary scattering length used in our calculations are within the expected limit for *p* type and HVPE samples of the given dimensions. We also find that considerable amount of extended defects are present in the sample. Our calculation for the presence of extended defects is supported by Sosnowska and Frymark.[32]

The temperature dependence beyond the conductivity peak for #2 and #3 [samples 5 and 6] is also different from experimental measurements for the other samples prepared and measured by other groups. To show the difference in the temperature dependence of the thermal conductivity with other experimental measurements, we have plotted the results of Jeżowski *et al.*[8] (sample #1) and Slack[7] in Fig. 5. We observe that the experimental results by Jeżowski *et al.*[8–10] (for sample #1) are higher than those by Slack *et al.*[7] in the temperature range $70 < T < 200$ K, the range where our the-

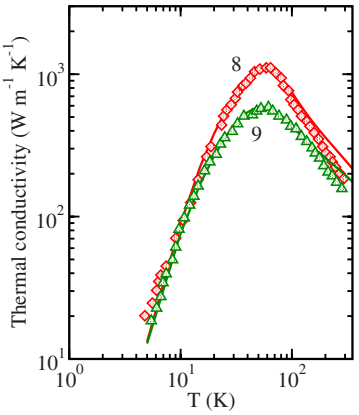

FIG. 6. (Color online) Temperature variation in the thermal conductivity of sample no. 8 and 9 from Jezowski *et al.* The solid lines represent our theoretical results and the symbols represent the experimental data presented in Ref. 10.

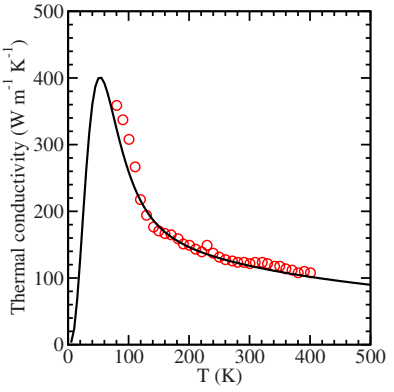

FIG. 7. (Color online) Temperature variation in the thermal conductivity of sample no. 10 from Liu and Balandin (Ref. 12). The solid lines represent our theoretical results and the symbols represent the experimental data presented in Ref. 12.

oretical results did not match with, i.e., are lower than, the experimental data by Jeżowski *et al.* Therefore, we believe that the experimental results by Jeżowski *et al.* may have been modified due to some artifacts. Table IV shows that for samples #2 and #3 [samples 5 and 6], point-defect scattering contributes at least 9% to thermal resistivity at 1000 K. Between 300 K and the Debye temperature, impurity-scatttering contribution is significant.

The reported characteristics of samples #2 and #3 in Refs. 9 and 10 [samples 8 and 9] suggested that they were not only identical to each other but also to sample #1 [sample 4]. The three samples have been grown under the same conditions using the same growth technique. They also had the same dimensions and the same impurities levels.[9,10] However, these samples exhibited different thermal-conductivity values. We have found from our calculations that different defect-scattering strengths had to be used in order to explain the reported conductivity spectrum of these samples. Thus, we ascribe the differences in the measured thermal conductivity to possible differences in the structure and distribution of impurities in these samples, in addition to possible differences in the concentrations of these impurities. For samples #2 and #3 in Refs. 9 and 10 [samples 8 and 9], the boundary limit for phonon mean-free path was found to be 100 μm, which is on the order of the smallest dimension of the samples. The results of the thermal conductivity of these two samples are shown in Fig. 6. The higher conductivity for sample #2 [sample 8] indicates that phonon-defect scattering in this is lower than that in sample #3 [sample 9]. Table II shows that sample #2 [sample 8] has much lower point impurity and extended defect concentration compared to sample #3 [sample 9]. Table IV shows that the contribution of point-impurity scattering in sample #2 [sample 8] is similar to that of other HVPE samples discussed earlier.

B. GaN films

The fourth sample (sample #4) in Ref. 8 [sample 7] consisted of two different HVPE films grown on bulk GaN substrate. Results for this sample are shown in Fig. 4. This sample shows a lower thermal conductivity compared to other samples studied in Ref. 8 throughout the whole temperature range, and it shows a clear deviation from the characteristic boundary T^3 dependence at low temperatures. This deviation can be attributed to the combination of strong grain-boundary scattering and scattering from very large extended defects as shown in Table II. Between room temperature and the Debye temperature, impurity-scattering contribution to the thermal resistivity is significant. This contribution is about 5% at 1000 K as shown in Table IV.

In Fig. 7, the thermal-conductivity results of the 18.5-μm-thick GaN film [sample 10] grown and studied by Liu and Balandin[12] are presented. The film was grown on the *c*-plane sapphire substrate by a modified HVPE technology. Since no measurements were taken below 80 K, we considered the boundary limit to be equal to the thickness of the sample (18.5 μm) in our calculations. In order to obtain the best fit with the experimental results, as displayed in Fig. 7, very high level of point-impurity concentration was chosen [see Table II]. The experimentally measured room-temperature thermal conductivity was 125 W m^{-1} K^{-1}, which is lower than that of bulk (in the range 130–230 W m^{-1} K^{-1}). Extended defects are found to be absent in the sample. We find that this sample does not contain any other types of defect, except point impurities. The contribution of impurity scattering toward the total thermal conductivity is found to be quite high throughout the whole temperature range studied here. Even at 1000 K, the point-impurity contribution to thermal resistivity is as high as 30%.

Figure 8 presents the results for the GaN sample grown by Luo *et al.* [sample 11]. This sample was grown using the LEO technique. This is the thinnest film sample studied in this work with sample thickness of 5 μm. Similar to the 18.5 μm film grown by Liu and Balandin,[12] this sample also contains only point defects. We find that the point-impurity concentration in this sample is low, with the impurity-scattering factor $A=10\times10^{-46}$ s^3 in Eq. (6). Though our numerical results at low-temperature range fits well with the experimental data, the fitting is poor beyond the conductivity peak. The experimental result from the third harmonic

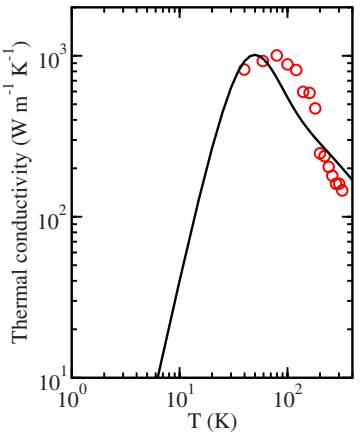

FIG. 8. (Color online) Temperature variation in the thermal conductivity of sample no. 11 (the LEO GaN sample). The solid lines represent our theoretical results and the symbols represent the experimental data presented in Ref. 5.

method was corrected for finite geometry effects. Interface effects are very important for determination of thermal conductivity of samples of such dimension. Effects of reflection of thermal waves from interfaces were corrected by invoking the presence of a series of image heat sources.[5] For the uncoalesced LEO structure, the simplest assumption is that the distance r is much shorter than thermal diffusion wavelength and it does not take into account the effect of multiple images. Table III in Ref. 5 shows that even in the case of five mirror images are taken into account, the image correction scheme does not converge to the analytical solution. Therefore, the simplest image correction scheme underestimates the thermal conductivity of the LEO sample. This may be one of the main reasons behind the poor fitting of our numerical result with the experimental data in the temperature range where the point-impurity scattering dominates. Moreover, we have used the continuum approximation in our theory. For such films, phonon-dispersion curves are likely to deviate significantly from the continuum relation employed here. Considerations of such changes may result in better fitting with experimental measurements both in the temperature range where phonon-impurity scattering and phonon-phonon scattering dominates. In the case of 5-μm-thick film also, similar consideration of deviation of phonon-dispersion relations from the continuum approximation is very likely to alter the contribution of phonon-impurity scattering and phonon-phonon scattering toward the overall thermal resistivity.

C. Comparison of results for films grown by different methods

As discussed previously, in this study we have investigated the thermal conductivity of three GaN films (samples 7, 10, and 11) grown using two techniques (HVPE and LEO). In Table V, the values of the thermal conductivity calculated at temperatures 77, 300, and 912 K (liquid nitrogen temperature, room temperature, and Debye temperature) have been presented. These results suggest that there is a huge spread of conductivity results at any low temperature. The room-temperature values range from 118 W m^{-1} K^{-1} (for the HVPE film) to 251 W m^{-1} K^{-1} (for the HT/HP bulk samples). We also note that at room temperature, sample 11 (the LEO film by Luo *et al.*[5]) shows a conductivity value of 211 W m^{-1} K^{-1} which is higher than that exhibited by some bulk samples. The other two film samples (samples 7 and 10) exhibited room-temperature conductivity values lower than that of bulk samples. These results are consistent with the knowledge that the LEO method produces materials with lower dislocation density compared to the HVPE method. Therefore, the room-temperature thermal-conductivity value of the LEO film is similar to that of thermal conductivity of bulk GaN.

The experimentally reported results along with our calculated results indicate that the thinnest film grown by Luo *et al.*[5] [sample 11] is more suitable than other films for high-temperature thermal device applications. This can be understood clearly, as high-temperature thermal-conductivity results for this sample are almost exclusively controlled by phonon anharmonic interactions, and are not affected by size and purity of samples.

Clearly, suitability for thermal applications depends on the processing (i.e., growth technique) of GaN films, as types and concentration of defects, as well as sample size, become increasingly important at room temperature and below.

TABLE V. Range of thermal-conductivity values for the various GaN samples studied here. The parameters used are taken from Table II.

Our sample numbering	Ref. (growth technique and sample type)	77 K	300 K	912 K(Θ_D)
1	7 (HVPE, bulk)	1098	233	85.4
3	6 (HVPE, bulk)	77.6	160.4	75.0
10	12 (HVPE, film)	335.2	118.3	60.1
7	8 #4(HVPE film on bulk GaN)	136.4	135.3	68.8
	8 (HT/HP)			
4	#1 (Bulk, n type)	1310.6	250.8	87.5
5	#2 (Bulk, p type)	1105.4	250.2	87.5
6	#3 (Bulk, p type)	497.4	179.8	76.9
11	4 (LEO, film)	756.6	211.4	82.3
2	2 (GaCl+NH_3, 950 °C, bulk)	154.6	180.4	78.7

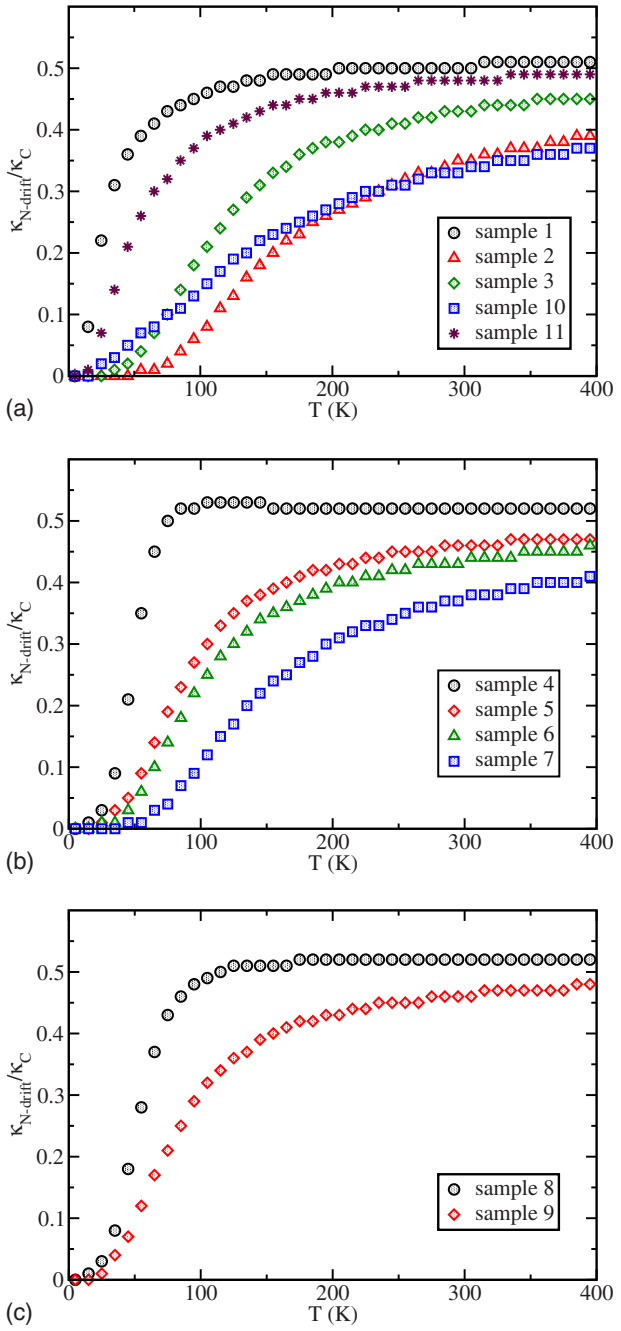

FIG. 9. (Color online) Contributions from the N-drift term toward the total thermal conductivity.

D. N-drift term

In Fig. 9 we present the contribution of the usually ignored N-drift term, $\kappa_{\text{N-drift}}$, to the total calculated thermal conductivity of the various samples studies in this work. We observe that the contribution of this term gradually decreases with increase in impurity concentration. However, the minimum contribution of the N-drift term to the total thermal conductivity at room temperature K was ~30% for the 18.5-μm-thick film grown by Liu and Balandin[12] [our sample number 10]. For samples with smaller amounts of defects, this contribution is as large as 50%, indicating that

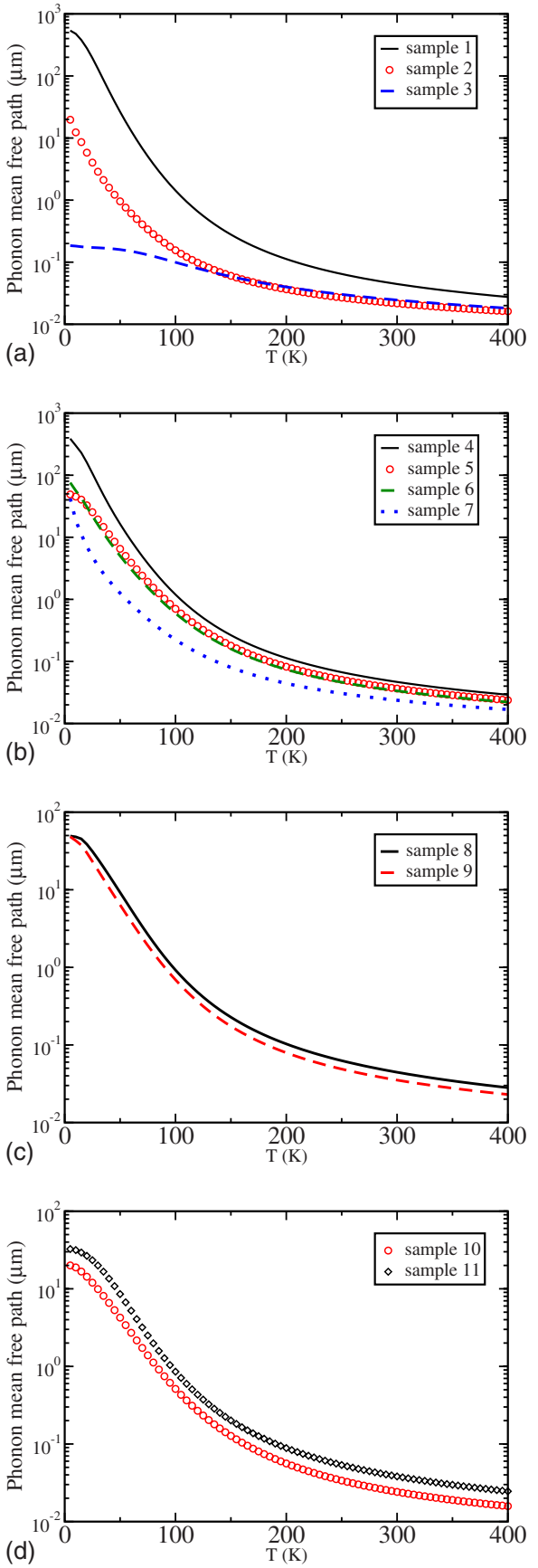

FIG. 10. (Color online) Phonon mean-free paths in the GaN samples studied in this work.

the N-drift term should not be ignored in theoretical studies of phonon transport in semiconductors.

E. Mode-average phonon mean-free path

Phonon mean-free paths in the eleven GaN samples studied in this work are shown in Fig. 10. Mode-average phonon mean-free path has been calculated using the following expression:[38]

$$\lambda = \frac{\sum_{\mathbf{q}s} \omega^2 c_s^2 \tau \bar{n}(\bar{n}+1)}{\bar{c}\sum_{\mathbf{q}s} \omega^2 \bar{n}(\bar{n}+1)} = \frac{\sum_s c_s^2 \int dx x^4 \tau \bar{n}(\bar{n}+1)}{\bar{c}\sum_s \int dx x^4 \bar{n}(\bar{n}+1)}, \quad (9)$$

where $\bar{c}$ is the average phonon speed and other symbols have been explained before. At room temperature, the mean-free path in the samples ranges between 20 and 40 nm. Due to the gradual dominance of anharmonicity with increase in temperature, the phonon mean-free path in all the samples starts to converge above room temperature. Above Debye temperature, phonon mean-free path reaches the same limit, with typical values in the range 7–9 nm at 1000 K. It can be seen that at low temperatures, the phonon mean-free path in most of the samples is limited by the boundary length. In some of the samples, the phonon mean-free path is lower (but of the same order) than our theoretically fitted boundary length. This is because the calculated phonon mean-free path in this work is the statistically mode-average mean-free path whereas the total phonon relaxation rate is in general the sum of contributions from various scattering processes. For some samples, at low temperatures, the phonon relaxation rate due to impurity scattering or grain-boundary scattering at some **q** points is nearly equal to or higher than the phonon relaxation rate due to boundary scattering. This results in an increased average relaxation rate and a smaller average mean-free path compared to that due to boundary scattering.

IV. SUMMARY

Using 11 samples (eight bulk and three films), a systematic theoretical investigation of the thermal conductivity of GaN grown under different growth techniques has been made over a large temperature range. Callaway's relaxation-time theory in its full form has been utilized, and calculations of the Debye term and N-drift term have been made by incorporating a detailed description for all allowed normal and umklapp three-phonon processes. Contributions of various phonon scatterings mechanisms in producing the wide range of thermal-conductivity results obtained for samples grown by different methods has been explained in a consistent manner. The analysis of results presented in this work indicates that for high-temperature thermal applications, GaN films grown by the LEO method can be considered as good as pure bulk GaN. It is found that impurity scattering plays a significant role in determining the thermal conductivity of all sample at room temperature and below, except for those containing very low contents of point impurities. For the samples studied, above room temperature, the contribution of the often ignored N-drift term in the Callaway's theory varies from 30% (for samples with large amounts of defects) to 50% (for samples with the minimum amount of defects).

ACKNOWLEDGMENT

Saswati Barman acknowledges the financial assistance (Grant No. SR/FTP/PS-71/2007) from the Department of Science and Technology, Government of India.

[1] G. A. Slack, J. Phys. Chem. Solids **34**, 321 (1973).
[2] E. K. Sichel and J. I. Pankove, J. Phys. Chem. Solids **38**, 330 (1977).
[3] V. M. Asnin, F. H. Pollak, J. C. Ramer, M. J. Schurman, and I. Ferguson, Appl. Phys. Lett. **75**, 1240 (1999).
[4] C. Y. Luo, H. Marchand, D. R. Clarke, and S. P. DenBaars, Appl. Phys. Lett. **75**, 4151 (1999).
[5] C. Luo, D. R. Clarke, and J. R. Dryden, J. Electron. Mater. **30**, 138 (2001).
[6] M. Kamano, M. Haraguchi, T. Niwaki, M. Fukui, M. Kuwahara, T. Okamoto, and T. Mukai, Jpn. J. Appl. Phys. **41**, 5034 (2002).
[7] G. A. Slack, L. J. Schowalter, D. Morelli, and J. A. Freitas, Jr., J. Cryst. Growth **246**, 287 (2002).
[8] A. Jeżowski, P. Stachowiak, T. Plackowski, T. Suski, S. Krukowski, M. Boćkowski, I. Grzegory, B. A. Danilchenko, and T. Paszkiewicz, Phys. Status Solidi B **240**, 447 (2003).
[9] A. Jeżowski, P. Stachowiak, T. Suski, S. Krukowski, M. Boćkowski, I. Grzegory, and B. Danilchenko, Physica B **329-333**, 1531 (2003).
[10] A. Jeżowski, B. A. Danilchenko, M. Boćkowski, I. Grzegory, S. Krukowski, T. Suski, and T. Paszkiewicz, Solid State Commun. **128**, 69 (2003).
[11] B. C. Daly, H. J. Maris, A. V. Nurmikko, M. Kuball, and J. Han, J. Appl. Phys. **92**, 3820 (2002).
[12] W. Liu and A. Balandin, Appl. Phys. Lett. **85**, 5230 (2004).
[13] A. Witek, Diamond Relat. Mater. **7**, 962 (1998).
[14] R. Berman, Diamond Relat. Mater. **8**, 2016 (1999).
[15] D. Kotchetkov, J. Zou, A. A. Balandin, D. I. Florescu, and F. H. Pollak, Appl. Phys. Lett. **79**, 4316 (2001).
[16] J. Zou, D. Kotchetkov, A. A. Balandin, D. I. Florescu, and F. H. Pollak, J. Appl. Phys. **92**, 2534 (2002).
[17] M. D. Kamatagi, N. S. Sankeshwar, and B. G. Mulimani, Diamond Relat. Mater. **16**, 98 (2007).
[18] M. Asen-Palmer, K. Bartkowski, E. Gmelin, M. Cardona, A. P. Zhernov, A. V. Inyushkin, A. Taldenkov, V. I. Ozhogin, K. M. Itoh, and E. E. Haller, Phys. Rev. B **56**, 9431 (1997).
[19] J. Callaway, Phys. Rev. **113**, 1046 (1959).
[20] G. P. Srivastava, Philos. Mag. **34**, 795 (1976).
[21] G. P. Srivastava, *The Physics of Phonons* (Adam Hilger, Bristol, 1990).
[22] S. Barman and G. P. Srivastava, Phys. Rev. B **73**, 073301 (2006).

[23] S. Barman and G. P. Srivastava, Phys. Rev. B **73**, 205308 (2006).
[24] A. AlShaikhi and G. P. Srivastava, J. Appl. Phys. **103**, 083554 (2008).
[25] P. G. Klemens, Proc. Phys. Soc., London, Ser. A **68**, 1113 (1955).
[26] J. W. Schwartz and C. T. Walker, Phys. Rev. **155**, 969 (1967).
[27] J. W. Vandersande, Phys. Rev. B **15**, 2355 (1977).
[28] J. E. Parrott, Rev. Int. Hautes Temp. Refract. **16**, 393 (1979).
[29] D. J. Ecsedy and P. G. Klemens, Phys. Rev. B **15**, 5957 (1977).
[30] X.-w. Sun, Z.-j. Liu, T. Song, X.-b. Liu, C.-w. Wang, and Q.-f. Chen, Chin. J. Chem. Phys. **20**, 233 (2007).
[31] S. Barman and G. P. Srivastava, Phys. Rev. B **69**, 235208 (2004).
[32] M. Lefeld-Sosnowska and I. Frymark, J. Phys. D **34**, A148 (2001).
[33] *Semiconductors*, Landolt-Börnstein, New Series, Group III Vol. 17, edited by O. Madelung, M. Sculz, and H. Weiss (Springer, Berlin, 1982).
[34] H. P. Maruska and J. J. Tietjen, Appl. Phys. Lett. **15**, 327 (1969).
[35] S. Porowski, J. Cryst. Growth **189-190**, 153 (1998).
[36] B. A. Danilchenko, I. A. Obukhov, T. Paszkiewicz, and A. Jeżowski, Solid State Commun. **144**, 114 (2007).
[37] C. Mion, J. F. Muth, E. A. Preble, and D. Hanser, Appl. Phys. Lett. **89**, 092123 (2006).
[38] J. M. Ziman, *Electrons and Phonons* (Oxford University Press, New York, 1967).